TGF-β1 mediates the hypertrophic cardiomyocyte growth induced by angiotensin II

See related Commentary on pages 715–716.

Jo El J. Schultz,[1,2] Sandra A. Witt,[3] Betty J. Glascock,[3] Michelle L. Nieman,[4] Peter J. Reiser,[5] Stacey L. Nix,[1] Thomas R. Kimball,[3] and Thomas Doetschman[1]

[1]Department of Molecular Genetics, Biochemistry, and Microbiology, and
[2]Department of Pharmacology and Cell Biophysics, Cincinnati College of Medicine, Cincinnati, Ohio, USA
[3]Noninvasive Cardiac Imaging and Hemodynamic Research Laboratory, Division of Cardiology, Department of Pediatrics, Children's Hospital Medical Center, Cincinnati, Ohio, USA
[4]Department of Molecular and Cellular Physiology, University of Cincinnati College of Medicine, Cincinnati, Ohio, USA
[5]Department of Oral Biology, The Ohio State University, Columbus, Ohio, USA

Address correspondence to: Jo El J. Schultz, Department of Pharmacology and Cell Biophysics, University of Cincinnati, College of Medicine, 231 Albert Sabin Way, ML 0575, Cincinnati, Ohio 45267, USA.
Phone: (513) 558-9754; Fax: (513) 558-1169; E-mail: schuljo@email.uc.edu.

Received for publication September 11, 2001, and accepted in revised form January 21, 2002.

Angiotensin II (Ang II), a potent hypertrophic stimulus, causes significant increases in *TGFb1* gene expression. However, it is not known whether there is a causal relationship between increased levels of TGF-β1 and cardiac hypertrophy. Echocardiographic analysis revealed that TGF-β1–deficient mice subjected to chronic subpressor doses of Ang II had no significant change in left ventricular (LV) mass and percent fractional shortening during Ang II treatment. In contrast, Ang II–treated wild-type mice showed a >20% increase in LV mass and impaired cardiac function. Cardiomyocyte cross-sectional area was also markedly increased in Ang II–treated wild-type mice but unchanged in Ang II–treated TGF-β1–deficient mice. No significant levels of fibrosis, mitotic growth, or cytokine infiltration were detected in Ang II–treated mice. Atrial natriuretic factor expression was ~6-fold elevated in Ang II–treated wild-type, but not TGF-β1–deficient mice. However, the α- to β-myosin heavy chain switch did not occur in Ang II–treated mice, indicating that isoform switching is not obligatorily coupled with hypertrophy or TGF-β1. The Ang II effect on hypertrophy was shown not to result from stimulation of the endogenous renin-angiotensis system. These results indicate that TGF-β1 is an important mediator of the hypertrophic growth response of the heart to Ang II.

J. Clin. Invest. **109**:787–796 (2002). DOI:10.1172/JCI200214190.

Introduction

TGF-β1 has activities important for the regulation of development, cell differentiation, tissue maintenance, and repair in a variety of cells and tissues (1, 2). Gene ablation of *Tgfb1* has demonstrated important roles for TGF-β1 in preimplantation development (3), yolk sac development (4), lymphocyte function (5–7), tooth development (8), genetic stability (9), platelet activation (10), and cancer (11–13). TGF-β1 is present in both cardiomyocytes and myocardial fibroblasts (14–18). In the heart, TGF-β1 has been shown to be expressed at high levels during cardiac development (19, 20) and pathology (2, 17, 18, 21). In fact, growth factors such as TGF-β1 and FGF-2 have been implicated in cardiomyocyte growth (16), fibrosis (22–24), and re-expression of the fetal isoforms of myofibrillar protein genes (25), all characteristics of hypertrophy. Recently, we have used *Fgf2* knockout mice to demonstrate that FGF-2 is required for a full hypertrophic response to high blood pressure, but that isoform switching is dependent upon high blood pressure rather than FGF-2 or hypertrophy (26).

Recent clinical evidence revealed that patients with idiopathic hypertrophic obstructive cardiomyopathy have elevated *Tgfb1* mRNA and protein levels localized to cardiomyocytes and TGF-β1 receptor levels found on both cardiomyocytes and fibroblasts (17, 18). Human atrial tissue stimulated with angiotensin II (Ang II) resulted in a significant increase in *Tgfb1* mRNA (24). Conversely, Tiret and colleagues (27) investigated eight candidate genes, including *Tgfb1*, in the susceptibility of idiopathic dilated cardiomyopathy and found that none of the polymorphisms were significantly associated with the risk or severity of the disease. Similarly, Patel and group (28) correlated functional variants of cardiac genes implicated in cardiac hypertrophy, including *Tgfb1*, with the severity of left ventricular (LV) hypertrophy in patients with hypertrophic cardiomyopathy. However, only TNF-α correlated with the indices of LV hypertrophy (28).

Other studies have demonstrated that Ang II, a potent hypertrophic stimulus, causes significant increases in *Tgfb1* expression. The Ang II–mediated increases in *Tgfb1* expression have been shown to correlate with cardiac hypertrophy (29), fibrosis (24, 30), and recapitulation of

fetal isoforms of cardiac myofibrillar proteins (31). Furthermore, cardiac hypertrophy and increased gene expression of *Tgfb1* and atrial natriuretic factor (*Anf*) have been demonstrated to be mediated by the Ang II type 1 (AT1) receptor (32). Recent work by Ichihara and colleagues (33) demonstrated that mice lacking the Ang II receptor (At_2) gene, when treated with pressor doses of Ang II, had no cardiac hypertrophy and had suppressed mRNA levels of *Tgfb1*, collagen I and III, and fibronectin. This group suggested that the loss of AT2 signaling attenuated the Ang II–induced gene expression of extracellular matrix (33). Nonetheless, it is not known whether there is a causal relationship between increased levels of *Tgfb1* and hypertrophy, isoform switching and fibrosis.

Our laboratory has generated a mouse that carries a targeted disruption in the *Tgfb1* gene (5). These mice have provided a valuable in vivo model to study the role of TGF-β1 in development, cardiovascular function, injury, and disease. *Tgfb1* knockout mice have a multifocal autoimmune-like inflammatory disease that leads to death by weaning age (5, 6). However, when these mice are bred onto an immune-compromised background, the inflammatory response is eliminated and the mice become useful for studying the effects of TGF-β1 in cardiac pathophysiological situations, including cardiac hypertrophy (7).

To examine whether TGF-β1 is essential for the development of cardiac hypertrophy, subpressor doses of Ang II were chronically administered for 4 weeks to $Tgfb1^{+/+}Rag1^{-/-}$ and $Tgfb1^{-/-}Rag1^{-/-}$ mice in the present study. Ang II was used instead of aortic banding because $Tgfb1^{-/-}$ mice are acutely sensitive to major surgical stress and rarely survive invasive surgery, due, in part, to the platelet aggregation defect that results in a doubling of bleeding time (10). For this reason, we used pharmacological treatment to induce hypertrophy. To avoid confusing the effects of Ang II with those of high blood pressure, we used chronic infusion of subpressor doses of Ang II. The results indicate that TGF-β1 is necessary for Ang II–mediated cardiac hypertrophy, but not for the re-expression of β-MHC protein, the fetal isoform of myosin heavy chain. The hypertrophic growth response of the heart occurred independently of an endogenously activated renin-angiotensin system (RAS), thereby demonstrating a direct action of TGF-β1 on cardiac remodeling.

Methods

$Tgfb1^{-/-}$ mice (5) were genetically combined with $Rag1^{-/-}$ mice (34) resulting in a colony with a mixed background of 129, CF1, and C57BL/6 (~2:1:1 ratios, respectively). Mice were housed in a specific pathogen-free facility and handled in accordance with standard use protocols and animal welfare regulations. All protocols were approved by the University of Cincinnati Institutional Animal Care and Use Committee.

$Tgfb1^{+/+}Rag1^{-/-}$ and $Tgfb1^{-/-}Rag1^{-/-}$ mice (6–8 weeks of age) were randomly assigned to the present study, and 11 $Tgfb1^{+/+}Rag1^{-/-}$ and ten $Tgfb1^{-/-}Rag1^{-/-}$ mice receiving Ang II and eight $Tgfb1^{+/+}Rag1^{-/-}$ and 6 $Tgfb1^{-/-}Rag1^{-/-}$ mice receiving saline completed the project, which included echocardiography, blood pressure measurements, histology/morphology, and *Anf* expression and MHC protein determination. Exclusion from the study was based on signs of distress (i.e., loss of body weight, lethargy) following implantation of the mini-pump. One $Tgfb1^{+/+}Rag1^{-/-}$ mouse and five $Tgfb1^{-/-}Rag1^{-/-}$ mice were excluded because of death or signs of morbidity.

Subcutaneous implantation of mini-osmotic pumps. $Tgfb1^{+/+}Rag1^{-/-}$ and $Tgfb1^{-/-}Rag1^{-/-}$ mice of either sex weighing 18–24 g were anesthetized intraperitoneally with 2.5% Avertin (2 mg/0.01 kg). Under sterile conditions, a midscapular incision was made. With the use of a dissecting stereoscope, a blunt dissection to spread the subcutaneous tissue, creating a pocket for the mini-osmotic pump, was performed. A mini-osmotic pump (ALZET, model 1002 or 2004; ALZA Corp., Palo Alto, California, USA) filled with saline or a subpressor dose of Ang II (100 ng/kg/min) was inserted underneath the skin. The incision was closed with 5-0 silk. The contents of the mini-osmotic pump were delivered into the local subcutaneous space at a rate of 0.25 μl/hour for 4 weeks. The mice were monitored daily for 4 weeks, noting body weight and water intake. The subpressor dose and delivery time of Ang II was based on preliminary, unpublished dose response data from our lab and published work by Harada and colleagues (35).

Echocardiography. Echocardiography was performed preoperatively and once a week postoperatively for 4 weeks on immunodeficient wild-type and *Tgfb1* knockout mice, as previously described (26). Intra- and inter-observer variability was similar to that previously noted in our laboratory (36). M-mode measurements of LV end-diastolic and end-systolic chamber size (LVED and LVES, respectively), septal wall thickness (SWT), LV posterior wall thickness (PWT) in diastole and systole, and R-R intervals were made from original tracings, as suggested by the American Society of Echocardiography (37). LV mass was estimated using the cube formula and cardiac function (fractional shortening, or FS) was calculated (26).

In vivo blood pressure measurements. Blood pressure measurements were obtained as described previously (26). Briefly, pretreated and 4-week saline- and Ang II–treated $Tgfb1^{+/+}Rag1^{-/-}$ and $Tgfb1^{-/-}Rag1^{-/-}$ mice of either sex were anesthetized with intraperitoneal injections of ketamine and inactin. A tracheotomy was performed to allow the mice to breathe spontaneously. A catheter was placed in the femoral artery for the measurement of systemic blood pressure. A Millar (1.4F) catheter (Millar Instruments Inc., Houston, Texas, USA) was placed in the right common carotid artery and advanced into the left ventricle for the measurement of left intraventricular pressure. Body temperature was maintained at 37°C using a thermally controlled surgical table and monitored with a rectal probe. The mice were then allowed to stabilize for 30 minutes prior to the blood pressure measurements.

Urine aldosterone and electrolyte analysis. Twenty-four–hour urine samples were obtained from

Tgfb1$^{+/+}$*Rag1*$^{-/-}$ and *Tgfb1*$^{-/-}$*Rag1*$^{-/-}$ mice before and after 4 weeks of saline or drug infusion. Extraction and determination of aldosterone levels in the urine were performed according to the Coat-A-Count aldosterone procedure (Diagnostic Products Corp., Los Angeles, California, USA). Hydrolysis of urine with 3.2 N HCl occurred overnight at room temperature in the dark, followed by an ethyl acetate extraction. To known standard and urine samples, 1 ml of ^{125}I aldosterone was added, and the samples were incubated for 18 hours at room temperature. Samples were counted for 1 minute in a gamma counter, and a standard calibration curve was produced. Aldosterone levels (picograms per milliliter) in the urine samples from *Tgfb1*$^{+/+}$*Rag1*$^{-/-}$ and *Tgfb1*$^{-/-}$*Rag1*$^{-/-}$ mice were determined from the standard calibration curve, and aldosterone concentration (micrograms per day) was calculated.

Electrolyte (Na^+ and K^+) levels were also determined from 24-hour urine samples obtained from *Tgfb1*$^{+/+}$*Rag1*$^{-/-}$ and *Tgfb1*$^{-/-}$*Rag1*$^{-/-}$ mice before and after 4 weeks of saline or drug infusion. Urine samples were diluted within the linear range for quantitation of Na^+ and K^+ levels by flame photometry (Corning model 480; Ciba Corning Diagnostics Corp., Medfield, Massachusetts, USA).

Cardiac myocyte staining. Morphological changes (i.e., myocyte cross-sectional area and longitudinal dimension) were measured by fluorescence staining of heart (left ventricle) sections from 4-week saline- and Ang II–treated *Tgfb1*$^{+/+}$*Rag1*$^{-/-}$ and *Tgfb1*$^{-/-}$*Rag1*$^{-/-}$ mice as previously described (26). Fluorescence-tagged wheat germ agglutinin was employed because it binds to saccharides of cellular membranes (38) and has been used by other investigators for the measurement of myocyte cross-sectional area (39). Images of LV cardiomyocyte cell membranes were captured digitally and analyzed using NIH Scion Image (version 1.62a).

Detection of Anf expression in the heart. Samples from the left ventricle of saline- and Ang II–treated *Tgfb1*$^{+/+}$*Rag1*$^{-/-}$ and *Tgfb1*$^{-/-}$*Rag1*$^{-/-}$ mice were prepared for real-time PCR employing RNA isolation and first-strand cDNA methods. Total RNA was isolated with RNAzol B (Tel-Test Inc., Friendswood, Texas, USA), following the manufacturer's instructions, with a final concentration of 1.3–2.9 μg/μl. RNA (7.5 μg) was transcribed into cDNA using oligo-dT (as the primer) and Superscript II Reverse Transcriptase (Life Technologies Inc., Rockville, Maryland, USA). The cDNA reaction was diluted to a final volume of 75 μl, and 1.5 μl from each sample was used for PCR amplification.

Real-time PCR (Smart Cycler model; Cepheid, Sunnyvale, California, USA) with the Light Cycler DNA Master SYBR Green I dye intercalation assay (Roche Molecular Biochemicals Inc., Indianapolis, Indiana, USA) was performed to detect the cardiac expression of *Anf* in saline- and Ang II–treated *Tgfb1*$^{+/+}$*Rag1*$^{-/-}$ and *Tgfb1*$^{-/-}$*Rag1*$^{-/-}$ mice as described previously (40). Primers were generated to murine *Anf* (upper 5′CCTGTGTACAGTGCGGTGTC3′ and lower 5′TGACCTCATCTTCTACCGGC3′; GenBank accession number K02781) to discriminate between products derived from cDNA and genomic DNA templates. The cDNA samples were subjected to real-time PCR, with an annealing temperature of 60°C, in which a 91-bp fragment of the *Anf* gene was amplified. Measurements were taken at the end of the 72°C extension step in each cycle, and the second derivative method was used to calculate the threshold cycle. Melt curve analysis showed a single sharp peak for all samples. *Arabidopsis thaliana* mRNA spiked into each RNA sample was used to control for efficiencies of the cDNA and PCR reactions.

The control (saline-treated wild-type) thresholds were averaged and this average was compared against the treatment groups of *Tgfb1*$^{+/+}$*Rag1*$^{-/-}$ and *Tgfb1*$^{-/-}$*Rag1*$^{-/-}$ mice. The threshold cycle differences correspond to the fold changes for *Anf* expression in the different groups.

Gel electrophoresis and protein separation of α-MHC and β-MHC. Samples from the left ventricle of saline- and Ang II–treated *Tgfb1*$^{+/+}$*Rag1*$^{-/-}$ and *Tgfb1*$^{-/-}$*Rag1*$^{-/-}$ mice were prepared for gel electrophoresis. The methods for sample preparation and for separation of α-MHC and β-MHC protein and quantification of the MHC isoforms were performed as described previously (26, 41).

Statistical analysis of data. All values are expressed as mean plus or minus SEM. Myocyte cross-sectional area, tissue weight/tibia length ratios, renin-angiotensin parameters (blood pressure, urine aldosterone, and Na^+ levels), *Anf* gene expression, and MHC protein levels were compared by Student *t* test. Differences between echocardiographic data, body weights, and water intake at various time points were compared using two-way ANOVA for time and treatment with repeated measures with Fisher's least significant difference test. Statistical differences were considered significant when *P* values were less than 0.05.

Results

Echocardiography was performed on *Tgfb1*$^{+/+}$*Rag1*$^{-/-}$ and *Tgfb1*$^{-/-}$*Rag1*$^{-/-}$ mice before and during the 4-week administration of a subpressor dose of Ang II (100 ng/kg/min). For all echocardiographic parameters studied, Ang II–treated mice were compared with saline-treated mice. Table 1 depicts the echocardiographic measurements of LV chamber size (LVED and LVES), SWT and PWT, heart rate (HR), stroke volume (SV), and cardiac output (CO) obtained before and during the time course of Ang II treatment. By 3 weeks of Ang II, both LVED and PWT were significantly higher in *Tgfb1*$^{+/+}$*Rag1*$^{-/-}$ mice, and by 4 weeks of Ang II, LVED and LVES were significantly elevated compared with pretreatment measurements ($P < 0.05$). At 4 weeks of Ang II, *Tgfb1*$^{+/+}$*Rag1*$^{-/-}$ mice had significantly higher echocardiographic dimensions of LVED, LVES, and SWT compared with 4-week Ang II–treated *Tgfb1*$^{-/-}$*Rag1*$^{-/-}$ ($P < 0.05$). No significant differences were observed in the echocardiographic measurements (LVES, LVED, SWT, and PWT) of *Tgfb1*$^{-/-}$*Rag1*$^{-/-}$ mice at any time point of the study. No significant changes in HR, SV, or CO were observed in Ang II–treated *Tgfb1*$^{+/+}$*Rag1*$^{-/-}$ and *Tgfb1*$^{-/-}$*Rag1*$^{-/-}$ mice compared with their pretreatment measures. Saline-treated *Tgfb1*$^{+/+}$*Rag1*$^{-/-}$ mice had no sig-

Table 1
Echocardiographic measures before and during 4 weeks of saline or Ang II (100 ng/kg/min) in *Tgfb1*$^{+/+}$*Rag1*$^{-/-}$ and *Tgfb1*$^{-/-}$*Rag1*$^{-/-}$ mice

		LVED	LVES	SWT	PWT	%FS	HR	SV	CO
Preinfusion	*Tgfb1*$^{+/+}$*Rag1*$^{-/-}$	3.55 ± 0.14	2.08 ± 0.11	0.73 ± 0.02	0.56 ± 0.03	42 ± 1	498 ± 31	0.034 ± 0.005	17.3 ± 3.3
	Tgfb1$^{-/-}$*Rag1*$^{-/-}$	3.45 ± 0.11	1.89 ± 0.15	0.68 ± 0.03	0.56 ± 0.01	46 ± 3	442 ± 17^{D}	0.026 ± 0.004	11.4 ± 1.4^{D}
1-week	*Tgfb1*$^{+/+}$*Rag1*$^{-/-}$	3.62 ± 0.18	2.19 ± 0.20	0.72 ± 0.06	0.64 ± 0.04	38 ± 3	472 ± 22	0.028 ± 0.004	13.5 ± 2.5
saline infusion	*Tgfb1*$^{-/-}$*Rag1*$^{-/-}$	2.96 ± 0.17^{A,B}	1.43 ± 0.09^{B}	0.61 ± 0.05	0.63 ± 0.03	52 ± 2^{A}	447 ± 24	0.023 ± 0.003	10.0 ± 1.1
1-week	*Tgfb1*$^{+/+}$*Rag1*$^{-/-}$	3.80 ± 0.22	2.42 ± 0.23	0.74 ± 0.05	0.55 ± 0.03	37 ± 4	522 ± 21^{B}	0.030 ± 0.003	15.7 ± 1.7
Ang II infusion	*Tgfb1*$^{-/-}$*Rag1*$^{-/-}$	3.54 ± 0.26^{C}	1.92 ± 0.13^{D}	0.64 ± 0.05	0.51 ± 0.02^{A,C}	45 ± 2^{D}	431 ± 19^{D}	0.027 ± 0.005	11.6 ± 1.6^{D}
2-week	*Tgfb1*$^{+/+}$*Rag1*$^{-/-}$	3.64 ± 0.21	2.16 ± 0.11	0.77 ± 0.05	0.57 ± 0.06	43 ± 0.3	478 ± 24	0.040 ± 0.006	19.4 ± 3.1
saline infusion	*Tgfb1*$^{-/-}$*Rag1*$^{-/-}$	3.12 ± 0.24^{B}	1.74 ± 0.19^{B}	0.76 ± 0.09	0.35 ± 0.02^{B}	45 ± 2	566 ± 43^{B}	0.023 ± 0.009	12.5 ± 3.6
2-week	*Tgfb1*$^{+/+}$*Rag1*$^{-/-}$	3.78 ± 0.20	2.28 ± 0.15	0.71 ± 0.06	0.62 ± 0.07	40 ± 1	438 ± 13^{A}	0.038 ± 0.008	17.1 ± 3.9
Ang II infusion	*Tgfb1*$^{-/-}$*Rag1*$^{-/-}$	3.48 ± 0.28	2.18 ± 0.16	0.68 ± 0 .06	0.52 ± 0.06^{C}	39 ± 2	429 ± 17	0.037 ± 0.008	16.0 ± 3.3
3-week	*Tgfb1*$^{+/+}$*Rag1*$^{-/-}$	3.60 ± 0.12	2.13 ± 0.14	0.68 ± 0.05	0.56 ± 0.03	43 ± 2	536 ± 33	0.029 ± 0.003	15.7 ± 2.2
saline infusion	*Tgfb1*$^{-/-}$*Rag1*$^{-/-}$	2.62 ± 0.36^{A,B}	1.35 ± 0.43^{B}	0.54 ± 0.03^{B}	0.47 ± 0.13	54 ± 10	496 ± 35	0.026 ± 0.001	12.9 ± 0.8
3-week	*Tgfb1*$^{+/+}$*Rag1*$^{-/-}$	3.95 ± 0.22^{A}	2.26 ± 0.20	0.77 ± 0.07	0.65 ± 0.05^{A,B}	43 ± 3	503 ± 38	0.038 ± 0.010	18.1 ± 3.7
Ang II infusion	*Tgfb1*$^{-/-}$*Rag1*$^{-/-}$	3.55 ± 0.32^{C}	2.01 ± 0.26	0.69 ± 0.07	0.64 ± 0.07	46 ± 3	445 ± 22	0.025 ± 0.001	11.0 ± 0.4^{D}
4-week	*Tgfb1*$^{+/+}$*Rag1*$^{-/-}$	3.68 ± 0.18	2.32 ± 0.15	0.74 ± 0.02	0.55 ± 0.03	43 ± 2	503 ± 24	0.038 ± 0.005	19.8 ± 2.6
saline infusion	*Tgfb1*$^{-/-}$*Rag1*$^{-/-}$	2.87 ± 0.24^{A,B}	1.22 ± 0.03^{B}	0.67 ± 0.02^{B}	0.48 ± 0.01^{B}	57 ± 3^{A}	414 ± 14^{B}	0.033 ± 0.006	13.7 ± 3.0
4-week	*Tgfb1*$^{+/+}$*Rag1*$^{-/-}$	3.85 ± 0.12^{A}	2.64 ± 0.11^{A,B}	0.76 ± 0.02	0.58 ± 0.03	32 ± 1^{A,B}	442 ± 34	0.040 ± 0.006	18.2 ± 3.4
Ang II infusion	*Tgfb1*$^{-/-}$*Rag1*$^{-/-}$	3.03 ± 0.55^{D}	1.51 ± 0.49^{D}	0.69 ± 0.02^{D}	0.59 ± 0.08	52 ± 5^{D}	415 ± 90	0.026 ± 0.010	11.6 ± 4.8

LVED, LVES, SWT (at end-diastole), PWT (at end-diastole) in millimeters. FS was determined from the echocardiographic measurements of LVED and LVES. HR, in beats per minute; SV, in milliliters; CO, in milliliters per minute. All values are represented as mean ± SEM. $^{A}P < 0.05$ vs. preinfusion cohort. $^{B}P < 0.05$ vs. *Tgfb1*$^{+/+}$*Rag1*$^{-/-}$ saline for same week. $^{C}P < 0.05$ vs. *Tgfb1*$^{-/-}$*Rag1*$^{-/-}$ saline for same week. $^{D}P < 0.05$ vs. *Tgfb1*$^{+/+}$*Rag1*$^{-/-}$ Ang II for same week.

nificant difference in echocardiographic measures at any time point. Cardiac function (%FS) was generally unchanged in Ang II–treated *Tgfb1*$^{-/-}$*Rag1*$^{-/-}$ mice, although %FS was significantly higher at 1 and 4 weeks of Ang II administration compared with *Tgfb1*$^{+/+}$*Rag1*$^{-/-}$ mice. Consequently, cardiac function was significantly diminished by 4 weeks of Ang II treatment in *Tgfb1*$^{+/+}$*Rag1*$^{-/-}$ mice, correlating with the increase in LV mass (see Figure 1a). This observation of impaired function in hypertrophic hearts supports our previous findings (26) and those of Ichihara and group (33). Table 2 shows the hemodynamic characteristics of *Tgfb1*$^{+/+}$*Rag1*$^{-/-}$ and *Tgfb1*$^{-/-}$*Rag1*$^{-/-}$ mice following 4 weeks of saline or Ang II treatment. HR and the rate of relaxation, –dP/dt, were not significantly different among the groups. However, Ang II–treated *Tgfb1*$^{-/-}$*Rag1*$^{-/-}$ mice had significantly lower mean blood pressure and LV pressure compared with saline-treated *Tgfb1*$^{-/-}$*Rag1*$^{-/-}$ mice and Ang II–treated *Tgfb1*$^{+/+}$*Rag1*$^{-/-}$ mice ($P < 0.05$). The rate of contraction, +dP/dt, was also significantly lower compared with Ang II–treated *Tgfb1*$^{+/+}$*Rag1*$^{-/-}$ mice ($P < 0.05$). The echocardiographic and hemodynamic indices of contractility did not correlate in this study; however, this finding was similar to other experimental and clinical studies comparing echocardiographic and catheterization analyses (42–45).

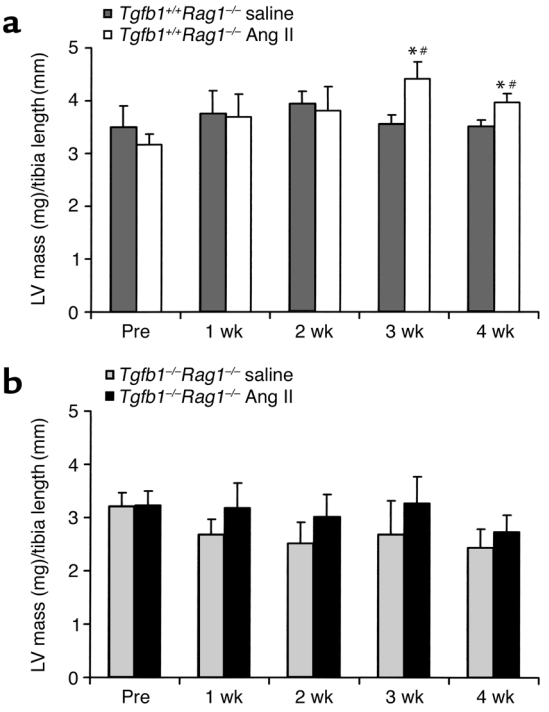

Figure 1
Serial echocardiographic results for *Tgfb1*$^{+/+}$*Rag1*$^{-/-}$ and *Tgfb1*$^{-/-}$*Rag1*$^{-/-}$ mice before and weeks during saline or subpressor Ang II treatment. LV mass was estimated from the echocardiographic measurements of SWT, PWT, and LVED. All values are expressed as mean ± SEM. *$P < 0.05$ vs. pre-Ang II. $^{\#}P < 0.05$ vs. *Tgfb1*$^{+/+}$*Rag1*$^{-/-}$. $n = 8$ for saline-treated *Tgfb1*$^{+/+}$*Rag1*$^{-/-}$ mice and $n = 6$ for saline-treated *Tgfb1*$^{-/-}$*Rag1*$^{-/-}$ mice. $n = 11$ for Ang II–treated *Tgfb1*$^{+/+}$*Rag1*$^{-/-}$ mice, and $n = 10$ Ang II–treated *Tgfb1*$^{-/-}$*Rag1*$^{-/-}$ mice. (**a**) Estimated LV mass for pretreatment and 1–4 weeks of saline-treated (dark gray bars) or Ang II–treated (white bars) *Tgfb1*$^{+/+}$*Rag1*$^{-/-}$ mice. By 3 weeks of subpressor Ang II treatment, a marked increase in LV mass was observed in *Tgfb1*$^{+/+}$*Rag1*$^{-/-}$ mice compared with their saline cohorts. (**b**) Estimated LV mass for pretreatment and 1–4 weeks of saline-treated (light gray bars) or Ang II–treated (black bars) *Tgfb1*$^{-/-}$*Rag1*$^{-/-}$ mice. No significant increase in LV mass was noted in Ang II–treated *Tgfb1*$^{-/-}$*Rag1*$^{-/-}$ mice compared with their saline cohorts.

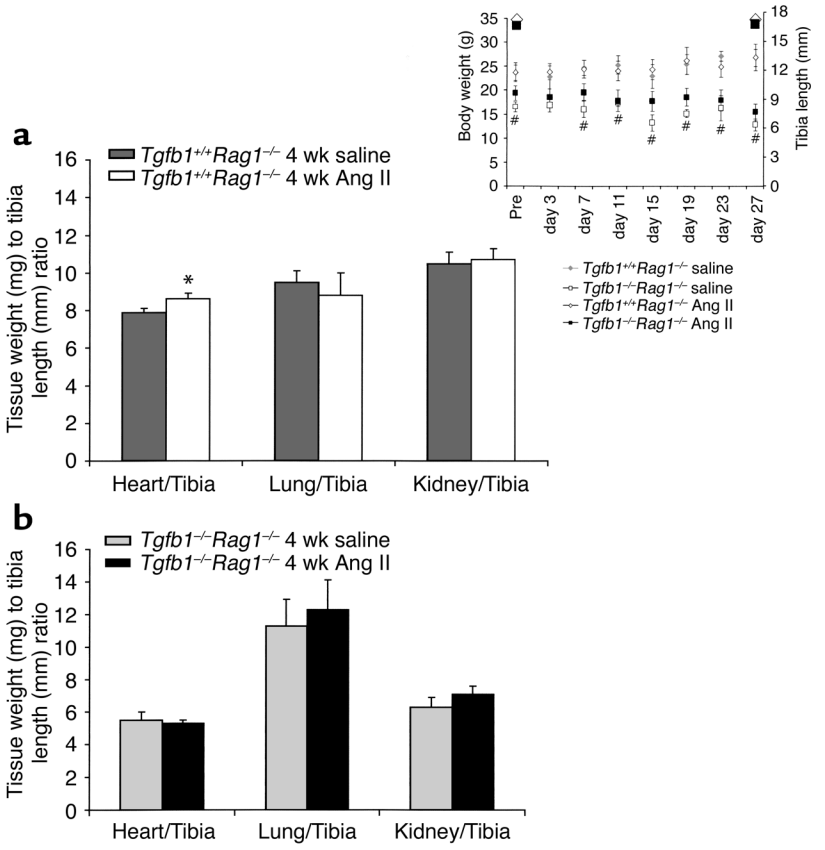

Figure 2
Tissue weight-to-tibia length ratios for 4-week saline- and Ang II–treated *Tgfb1*$^{+/+}$*Rag1*$^{-/-}$ and *Tgfb1*$^{-/-}$*Rag1*$^{-/-}$ mice. All values are expressed as mean ± SEM. *P < 0.05 vs. saline treatment. n = 8 for saline-treated *Tgfb1*$^{+/+}$*Rag1*$^{-/-}$ mice, and n = 6 for saline-treated *Tgfb1*$^{-/-}$*Rag1*$^{-/-}$ mice. n = 11 for Ang II–treated *Tgfb1*$^{+/+}$*Rag1*$^{-/-}$ mice, and n = 10 for Ang II–treated *Tgfb1*$^{-/-}$*Rag1*$^{-/-}$ mice. (**a**) Ang II–treated *Tgfb1*$^{+/+}$*Rag1*$^{-/-}$ mice (white bars) had a significant increase in heart/tibia ratio compared with the saline-treated mice (dark gray bars). (**b**) No significant difference in heart/tibia was observed in 4-week saline-treated (light gray bars) and Ang II–treated *Tgfb1*$^{-/-}$*Rag1*$^{-/-}$ mice (black bars). Inset: Graph depicting changes in body weight (small symbols) and tibia length (large symbols) in saline- and Ang II–treated *Tgfb1*$^{+/+}$*Rag1*$^{-/-}$ and *Tgfb1*$^{-/-}$*Rag1*$^{-/-}$ mice. Saline-treated *Tgfb1*$^{+/+}$*Rag1*$^{-/-}$ mice, filled diamonds. Saline-treated *Tgfb1*$^{-/-}$*Rag1*$^{-/-}$ mice, open squares. Ang II–treated *Tgfb1*$^{+/+}$*Rag1*$^{-/-}$ mice, open diamonds. Ang II–treated *Tgfb1*$^{-/-}$*Rag1*$^{-/-}$ mice, filled squares. Body weight was significantly lower in *Tgfb1*$^{-/-}$*Rag1*$^{-/-}$ mice compared with *Tgfb1*$^{+/+}$*Rag1*$^{-/-}$ mice and continued to decrease during the course of the study, whereas tibia length for both groups of mice was similar.

Figure 1, a and b, illustrates the estimated LV mass for saline- and Ang II–treated *Tgfb1*$^{+/+}$*Rag1*$^{-/-}$ and *Tgfb1*$^{-/-}$*Rag1*$^{-/-}$ mice. No significant increase in LV mass was observed in *Tgfb1*$^{-/-}$*Rag1*$^{-/-}$ mice during the course of Ang II administration compared with their pretreatment measurement or saline-treated *Tgfb1*$^{-/-}$*Rag1*$^{-/-}$ mice (Figure 1b). Three and 4 weeks of chronic Ang II treatment resulted in a statistically significant degree of cardiac hypertrophy (20–28%) in *Tgfb1*$^{+/+}$*Rag1*$^{-/-}$ mice compared with their pretreatment LV mass or saline-treated *Tgfb1*$^{+/+}$*Rag1*$^{-/-}$ mice and Ang II–treated *Tgfb1*$^{-/-}$*Rag1*$^{-/-}$ mice for the same time points (Figure 1a, P < 0.05). There was no significant change in LV mass or in LV dimensions in *Tgfb1*$^{+/+}$*Rag1*$^{-/-}$ and *Tgfb1*$^{-/-}$*Rag1*$^{-/-}$ mice during the course of saline treatment compared with their pretreatment measurements.

Gravimetrically, *Tgfb1*$^{-/-}$*Rag1*$^{-/-}$ mice had no significant increase in heart weight (HW) normalized to tibia length compared with their age- and sex-matched 4-week saline-treated cohorts (Figure 2). Similar to the echocardiographic analysis, HW/tibia length of *Tgfb1*$^{+/+}$*Rag1*$^{-/-}$ mice was increased significantly following Ang II administration (P < 0.05). There were no changes in lung or kidney weights in the Ang II–treated *Tgfb1*$^{+/+}$*Rag1*$^{-/-}$ and *Tgfb1*$^{-/-}$*Rag1*$^{-/-}$ mice compared with their saline-treated cohorts, indicating an absence of pulmonary edema and heart failure. Before any treatment, as well as during the course of the study, significant differences in body weight and organ weight (~1.3-fold less in knockout mice) were observed between *Tgfb1*$^{+/+}$*Rag1*$^{-/-}$ and *Tgfb1*$^{-/-}$*Rag1*$^{-/-}$ mice (see inset of Figure 2), although tibia length between the two groups was not different (17.2 ± 0.3 mm vs. 16.6 ± 0.3 mm, respectively; see inset). Body weight was not significantly altered in saline- or Ang II–treated *Tgfb1*$^{+/+}$*Rag1*$^{-/-}$ mice during the course of the study (see inset). Since after 1 week of age the knockout mice gain weight at a slower rate than their wild-type littermates and often begin losing weight after 15 days of age (5, 7, 46), tibia length, which did not change throughout the experiment, was used to normalize against the organ weight. The increase in HW in Ang II–treated *Tgfb1*$^{+/+}$*Rag1*$^{-/-}$ mice

Table 2
Hemodynamics of *Tgfb1*$^{+/+}$*Rag1*$^{-/-}$ and *Tgfb1*$^{-/-}$*Rag1*$^{-/-}$ mice following 4 weeks of saline or Ang II treatment

	Tgfb1$^{+/+}$*Rag1*$^{-/-}$		*Tgfb1*$^{-/-}$*Rag1*$^{-/-}$	
	Saline	Ang II	Saline	Ang II
HR	433 ± 11	427 ± 12	436 ± 15	429 ± 25
MAP	80 ± 8	78 ± 5	79 ± 3	63 ± 5[A,B]
LVP	110 ± 10	110 ± 7	100 ± 4	86 ± 2[A,B]
+dP/dt	10,369 ± 991	9,819 ± 594	9,048 ± 959	7,697 ± 646[B]
–dP/dt	–10,311 ± 1,401	–9,163 ± 576	–9,719 ± 1,003	–8,358 ± 760

HR, beats per minute. MAP and LVP in millimeters of mercury. +dP/dt and –dP/dt in millimeters of mercury per second. All values are represented as mean ± SEM. MAP, mean arterial blood pressure. [A]P < 0.05 vs. saline-treated *Tgfb1*$^{-/-}$*Rag1*$^{-/-}$ mice. [B]P < 0.05 vs. Ang II–treated *Tgfb1*$^{+/+}$*Rag1*$^{-/-}$ mice.

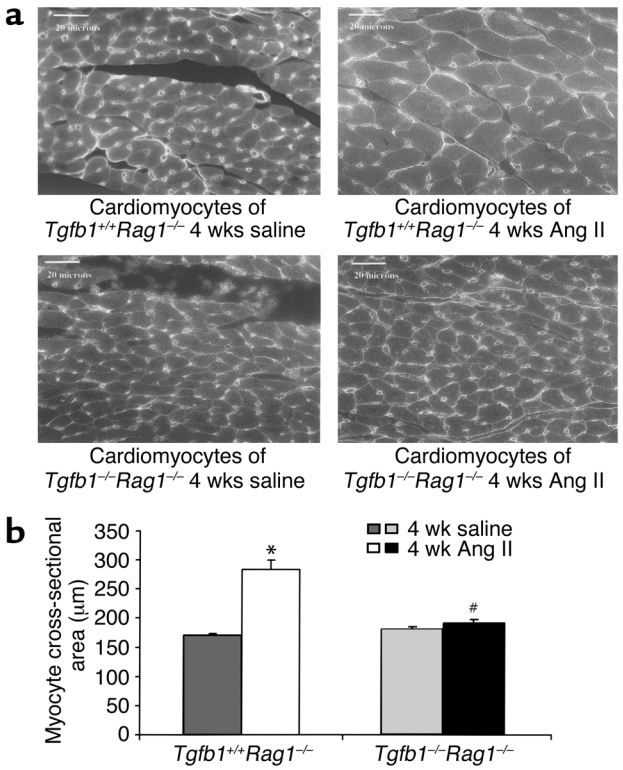

Figure 3
(**a**) Representative images of hearts from 4-week saline- and Ang II–treated *Tgfb1*$^{+/+}$*Rag1*$^{-/-}$ and *Tgfb1*$^{-/-}$*Rag1*$^{-/-}$ mice. Four-week Ang II–treated *Tgfb1*$^{+/+}$*Rag1*$^{-/-}$ heart depicting an increase in cardiomyocyte size. ×500. Scale bar, 20 μm. (**b**) Cardiomyocyte cross-sectional area of 4-week Ang II–treated *Tgfb1*$^{+/+}$*Rag1*$^{-/-}$ mice was significantly increased compared with saline-treated *Tgfb1*$^{+/+}$*Rag1*$^{-/-}$ and saline- or Ang II–treated *Tgfb1*$^{-/-}$*Rag1*$^{-/-}$ mice. Each column represents approximately 100 myocytes from each of four to five hearts per group. $^{*}P < 0.05$ vs. 4-week saline. $^{\#}P < 0.05$ vs. *Tgfb1*$^{+/+}$*Rag1*$^{-/-}$ 4-week Ang II.

is probably not the result of cardiac volume overload or tissue edema since the lung and kidney weights of this group are not different between saline treatment or Ang II treatment (Figure 2).

Morphological changes in LV cardiomyocytes from 4-week saline- and Ang II–treated *Tgfb1*$^{+/+}$*Rag1*$^{-/-}$ and *Tgfb1*$^{-/-}$*Rag1*$^{-/-}$ mice are represented in Figure 3a. Although HW/tibia length ratio is smaller in knockout compared with wild-type mice, the myocyte size is similar between the two groups, suggesting fewer cells in *Tgfb1*$^{-/-}$*Rag1*$^{-/-}$ mice. Morphometric analysis showed that *Tgfb1*$^{-/-}$*Rag1*$^{-/-}$ mice had no change in cardiomyocyte cross-sectional area following Ang II administration, whereas 4-week Ang II–treated *Tgfb1*$^{+/+}$*Rag1*$^{-/-}$ mice had a significant increase in myocyte cross-sectional area ($P < 0.05$; Figure 3b). These data are consistent with the echocardiographic and gravimetrical results and unequivocally demonstrate an in vivo role of TGF-β1 in the hypertrophic growth response of the heart. The longitudinal dimension of the cardiomyocytes were similar for saline- and Ang II–treated *Tgfb1*$^{+/+}$*Rag1*$^{-/-}$ and *Tgfb1*$^{-/-}$*Rag1*$^{-/-}$ mice (155 ± 4 μm for saline-treated wild-type, 165 ± 21 μm for saline-treated knockout, 135 ± 16 μm for Ang II–treated wild-type, and 132 ± 16 μm for Ang II–treated knockout mice), which indicates that the mice were not subjected to a volume overload from the treatment protocols.

Histological analysis via Masson's trichrome stain revealed only mild perivascular fibrosis in both *Tgfb1*$^{+/+}$*Rag1*$^{-/-}$ and *Tgfb1*$^{-/-}$*Rag1*$^{-/-}$ mice following 4 weeks of saline or subpressor Ang II dose (Figure 4a). Digital images (×25) of the entire left ventricle from saline- and Ang II–treated *Tgfb1*$^{+/+}$*Rag1*$^{-/-}$ and *Tgfb1*$^{-/-}$*Rag1*$^{-/-}$ mice were obtained using NIH Scion Image (version 1.62a). A 20 × 20 grid was superimposed over each image, and the number of points overlaying the Masson's Trichrome blue–stained interstitial fibrosis was counted. The percentage of cardiac fibrosis was determined as fibrosis points/left ventricle total points. There was no significant increase in the percentage of cardiac fibrosis in Ang II–treated *Tgfb1*$^{+/+}$*Rag1*$^{-/-}$ and *Tgfb1*$^{-/-}$*Rag1*$^{-/-}$ mice compared with saline-treated mice (Figure 4b).

To confirm that changes in LV mass were the result of cardiomyocyte hypertrophy, 4-week saline- and Ang II–

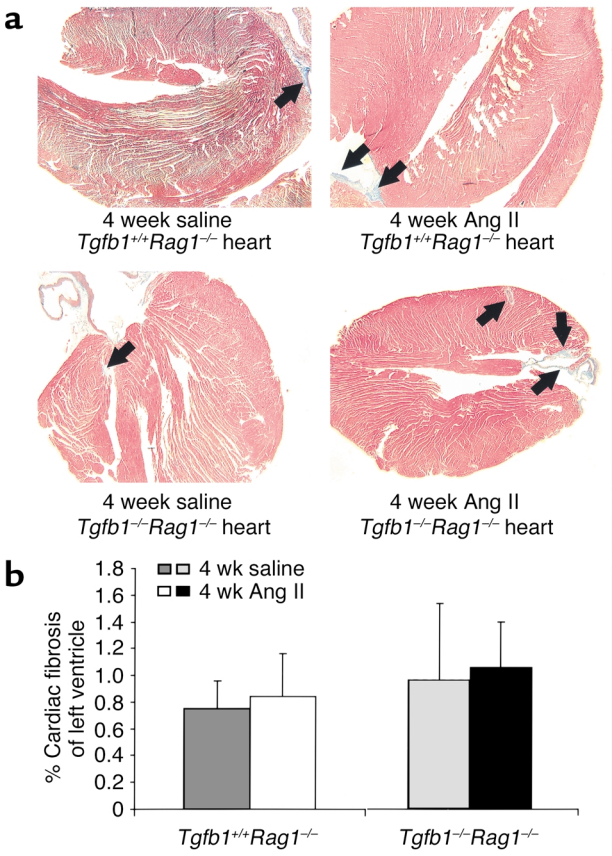

Figure 4
(**a**) Representative images of fibrotic lesions (black arrows) from 4-week saline- and Ang II–treated *Tgfb1*$^{+/+}$*Rag1*$^{-/-}$ and *Tgfb1*$^{-/-}$*Rag1*$^{-/-}$ mice. ×25. (**b**) Percentage of cardiac fibrosis in 4-week saline- and Ang II–treated *Tgfb1*$^{+/+}$*Rag1*$^{-/-}$ and *Tgfb1*$^{-/-}$*Rag1*$^{-/-}$ mice. Each column represents four to five hearts per group.

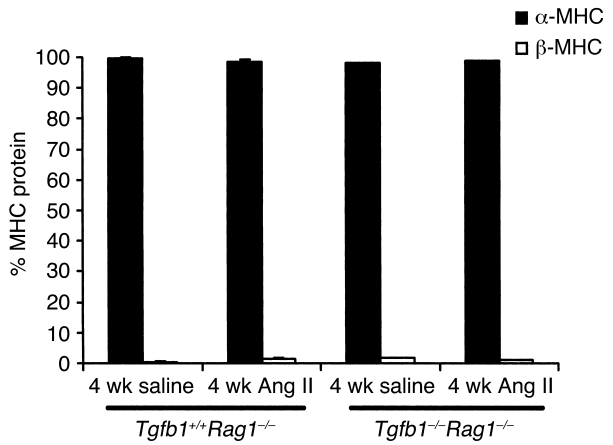

Figure 5
Expression pattern of MHC protein levels in saline- and Ang II–treated *Tgfb1*$^{+/+}$*Rag1*$^{-/-}$ and *Tgfb1*$^{-/-}$*Rag1*$^{-/-}$ mice. n = 5 for saline- and Ang II–treated *Tgfb1*$^{+/+}$*Rag1*$^{-/-}$ mice, and n = 4 for saline- and Ang II–treated *Tgfb1*$^{-/-}$*Rag1*$^{-/-}$ mice. Saline- and Ang II–treated *Tgfb1*$^{+/+}$*Rag1*$^{-/-}$ and *Tgfb1*$^{-/-}$*Rag1*$^{-/-}$ mice have similar levels of α-MHC (black bars) and β-MHC (white bars) protein. The cardiac hypertrophy observed in 4-week Ang II–treated *Tgfb1*$^{+/+}$*Rag1*$^{-/-}$ mice did not induce a re-expression of β-MHC.

treated *Tgfb1*$^{+/+}$*Rag1*$^{-/-}$ and *Tgfb1*$^{-/-}$*Rag1*$^{-/-}$ mice were injected with bromodeoxyuridine (BrdU) to observe any mitotic growth of the heart. No BrdU incorporation was detected in LV myocytes and nonmyocytes of saline- or Ang II–treated *Tgfb1*$^{+/+}$*Rag1*$^{-/-}$ and *Tgfb1*$^{-/-}$*Rag1*$^{-/-}$ mice (data not shown). Proliferating colonic epithelium taken as positive control from the same mice showed high levels of BrdU incorporation as expected (data not shown).

Since targeted disruption of the *Tgfb1* gene resulted in an autoimmune-like disorder, causing multiorgan inflammation and postnatal death by the age of 15–36 days (5, 6, 46, 47), TGF-β1–deficient mice were bred on an immune-compromised, RAG1-deficient background. These mice are still susceptible to infection. Therefore, to ensure that changes in LV mass were not due to mixed inflammatory cell infiltration into the heart, immunohistochemical detection of macrophages and neutrophils was performed. No macrophages or neutrophils were detected in the hearts of 4-week saline- and Ang II–treated *Tgfb1*$^{+/+}$*Rag1*$^{-/-}$ and *Tgfb1*$^{-/-}$*Rag1*$^{-/-}$ mice (data not shown). These results demonstrate that it was not fibrosis, cellular hyperplasia, or cytokine infiltration, but rather hypertrophy that was the cause of the LV mass increase in *Tgfb1*$^{+/+}$*Rag1*$^{-/-}$ mice.

The known biological actions of angiotensin II include vasoconstriction, triggering the thirst center in the brain and stimulation of aldosterone release from the adrenal glands (48–50). Subpressor doses of Ang II were used in the present study to examine the hypertrophic effects of TGF-β1 independent of a hemodynamic load. Therefore, to confirm that the cardiac remodeling response to Ang II administration was not the result of a pressure or volume overload, blood pressure, daily water intake, and urine aldosterone and Na^+ levels were measured. Systemic blood pressure (*Tgfb1*$^{+/+}$*Rag1*$^{-/-}$ pretreatment 85 ± 7 mmHg vs. 4-week saline 80 ± 8 mmHg vs. 4-week Ang II 78 ± 5 mmHg) and daily water intake (*Tgfb1*$^{+/+}$*Rag1*$^{-/-}$ pretreatment 5.1 ± 0.6 ml/day vs. 4-week saline 6.4 ± 0.9 ml/day vs. 4-week Ang II 5.8 ± 0.8 ml/day; *Tgfb1*$^{-/-}$*Rag1*$^{-/-}$ pretreatment 5.8 ± 1.0 ml/day vs. 4-week saline 5.9 ± 1.4 ml/day vs. 4-week Ang II 4.7 ± 0.8 ml/day) were not different before treatment or in saline- and Ang II–treated mice. The amount of Na^+ absorption versus excretion is a measure of aldosterone activity and indicates a stimulated renin-angiotensin system (51, 52). Urinary Na^+ levels (*Tgfb1*$^{+/+}$*Rag1*$^{-/-}$ pretreatment 0.12 ± 0.04 mmol/day vs. 4-week saline 0.10 ± 0.02 mmol/day vs. 4-week Ang II 0.13 ± 0.07 mmol/day; *Tgfb1*$^{-/-}$*Rag1*$^{-/-}$ pretreatment 0.10 ± 0.03 mmol/day vs. 4-week saline 0.08 ± 0.03 mmol/day vs. 4-week Ang II 0.05 ± 0.02 mmol/day) as well as K^+ levels (unpublished data) were similar between *Tgfb1*$^{+/+}$*Rag1*$^{-/-}$ and between *Tgfb1*$^{-/-}$*Rag1*$^{-/-}$ mice before and after saline or Ang II treatment, indicating that endogenous RAS was not activated by 4-week subpressor Ang II administration. Urine aldosterone levels were also measured. There was no significant difference in aldosterone levels between saline- and Ang II–treated *Tgfb1*$^{+/+}$*Rag1*$^{-/-}$ mice (0.005 ± 0.001 μg/day vs. 0.009 ± 0.003 μg/day, respectively), demonstrating that the dose of Ang II used did not stimulate a significant release of aldosterone. Following 4-week saline treatment, urine aldosterone was markedly increased in *Tgfb1*$^{-/-}$*Rag1*$^{-/-}$ mice compared with Ang II–treated *Tgfb1*$^{-/-}$*Rag1*$^{-/-}$ mice (0.007 ± 0.001 μg/day vs. 0.004 ± 0.001 μg/day, respectively; $P < 0.05$). Nonetheless, these electrolyte and aldosterone data along with the blood pressure and water intake measurements indicate that the endogenous RAS was not activated at this dose of Ang II and suggest that neither a pressure overload or volume overload has occurred in this model.

Re-expression of fetal isoforms of myofibrillar protein genes, including that for β-MHC, has been used as a biomarker for cardiac hypertrophy. Growth factors such as TGF-β1 have been demonstrated to stimulate this recapitulation of fetal cardiac genes (25, 31). There was 97–99% α-MHC and 1–3% β-MHC protein in 4-week saline-treated *Tgfb1*$^{+/+}$*Rag1*$^{-/-}$ and *Tgfb1*$^{-/-}$*Rag1*$^{-/-}$ mice (Figure 5). Following 4 weeks of Ang II treatment, *Tgfb1*$^{+/+}$*Rag1*$^{-/-}$ mice, which had cardiac hypertrophy, and *Tgfb1*$^{-/-}$*Rag1*$^{-/-}$ mice, which had not undergone a hypertrophic growth response, had similar α- and β-MHC protein levels as saline-treated mice (Figure 5), indicating that changes in the protein isoforms of MHC are not coupled to hypertrophy or TGF-β1.

Induction of the atrial natriuretic factor (*Anf*) gene is a response that occurs during cardiac hypertrophy (see review, ref. 53) and may represent a molecular marker that differentiates between physiological and pathological hypertrophy (54, 55). *Anf* expression increased approximately sixfold ($P < 0.05$, n = 5) following Ang II treatment in *Tgfb1*$^{+/+}$*Rag1*$^{-/-}$ mice compared with saline-treated cohorts (n = 5). These changes in *Anf* expression correlate with the induction of the hypertrophic

response of the *Tgfb1*$^{+/+}$*Rag1*$^{-/-}$ heart. There was a no-fold increase in Ang II–treated *Tgfb1*$^{-/-}$*Rag1*$^{-/-}$ mice (n = 4) compared with their saline-treated cohorts (n = 4).

Discussion

This is the first direct evidence to our knowledge to demonstrate a functional role of TGF-β1 in the hypertrophic response of the heart. Echocardiographic, gravimetric, and morphologic analyses clearly demonstrate that an absence of TGF-β1 results in no cardiac hypertrophy in response to Ang II treatment (Figure 1b, Figure 2, and Figure 3). The hypertrophic response occurs independent of the hemodynamic (pressure and volume load alterations) effects of Ang II, a potent hypertrophic stimulus, because blood pressure, thirst stimulation, and urine aldosterone and Na^+ levels were not increased compared with saline treatment. Interestingly, re-expression of β-MHC was not observed, suggesting that isoform switching occurs independently of cardiac hypertrophy or TGF-β1. This is consistent with the findings of our cardiac hypertrophy study using FGF-2–deficient mice in which we demonstrated little hypertrophy in the absence of FGF-2 (26). In that study, high blood pressure was used to induce hypertrophy, and an isoform switch occurred in the presence of pressure overload, independently of the presence or absence of hypertrophy or of FGF-2. In the present study, *Anf* message levels were elevated in Ang II–treated wild-type mice relative to saline-treated wild-type mice, but *Anf* levels were not elevated in Ang II–treated *Tgfb1*$^{-/-}$*Rag1*$^{-/-}$ mice relative to saline-treated knockout mice, indicating that increased *Anf* expression correlates with the hypertrophic response of the heart and not with pressure or volume overload.

A number of studies have demonstrated that mRNA levels of *Tgfb1* are markedly increased upon pressure overload or pharmacological manipulation and correlated these mRNA changes to hypertrophic growth (16), fibrosis (23), and recapitulation of fetal cardiac myofibrillar protein genes (25). TGF-β1 has been shown to be secreted from cultured cardiomyocytes and fibroblasts during cyclic stretch (56). In fact, TGF-β1 has been a candidate mediator for the cardiac remodeling activities of Ang II (24, 29–33). Ang II stimulated cardiomyocyte hypertrophy by paracrine release of TGF-β1 from cardiac fibroblasts in a neonatal rat cell culture model (29). Ang II increased *Tgfb1* expression in cardiac fibroblasts that may act as an autocrine/paracrine stimulus for collagen formation (30) and may be mediated by the AT2 receptor (33). Everett and colleagues (32) showed that cardiac hypertrophy and increased gene expression of *Tgfb1* and *Anf* were mediated by the AT1 receptor. Ang II, via AT1 receptor, caused hypertrophy of cardiomyocytes and hyperplasia of nonmyocytes in culture and induced the protein expression of ANF, α-skeletal actin, and TGF-β1 in cardiac myocytes (31). Conversely, TGF-β1 did not appear to be involved in the Ang II–induced hypertrophic response of cultured neonatal cardiomyocytes (57). Nonetheless, most in vitro and in vivo studies have only demonstrated a correlative relationship between cardiac hypertrophy and TGF-β1. Our present study demonstrates a direct effect and a primary, functional role of TGF-β1 in the growth response of the heart during pharmacological stress. Our results support the previously reported clinical correlations demonstrating TGF-β1's role in cardiac hypertrophy (17, 18, 24).

One could argue that the absence of a hypertrophic response in Ang II–treated *Tgfb1*$^{-/-}$*Rag1*$^{-/-}$ mice may be due to an altered load on the heart. However, as judged by the similar water intake and urinary electrolyte and aldosterone levels of *Tgfb1*$^{+/+}$*Rag1*$^{-/-}$ vs. *Tgfb1*$^{-/-}$*Rag1*$^{-/-}$ mice, it is unlikely that volume overload is a major factor. It was observed that Ang II–treated *Tgfb1*$^{-/-}$*Rag1*$^{-/-}$ mice had an unexplained decrease in blood pressure (BP), and no hypertrophic response resulted from Ang II treatment. However, there is recent evidence by Knowles and colleagues (58) that uncouples cardiac hypertrophy and BP. This group showed that mice deficient in the ANF receptor A have cardiac hypertrophy under normal conditions and that chronic antihypertensive treatment (from 20 days to 4 months of age) to lower BP, below that of normal levels of wild-type mice, did not reduce their cardiac hypertrophy. Furthermore, this group coarcted these mice to generate pressure overload, which resulted in an enhanced hypertrophic response. They determined that the total cardiac load between wild-type and knockout mice was similar, but for any pressure load the knockout mice had an increased hypertrophic response, indicating that this effect is not simply a function of BP. This suggests that in our study it is the absence of TGF-β1 and not low BP that results in no hypertrophy.

Although we have shown that TGF-β1 is involved in cardiomyocyte hypertrophy during Ang II treatment, we did not detect any significant difference in the level of fibrotic lesions in *Tgfb1*$^{+/+}$*Rag1*$^{-/-}$ vs. *Tgfb1*$^{-/-}$*Rag1*$^{-/-}$ mice (Figure 4). Omura and group (59) demonstrated that alterations in levels of *Tgfb1* mRNA did not correlate with the increased mRNA expression of fibronectin and collagen I and III during low-dose isoprenaline, suggesting that cardiac fibrosis is probably not mediated by TGF-β1. Also, Boivin and colleagues (46) observed significant levels of perivascular and multifocal fibrosis in the hearts and livers of immunocompetent TGF-β1–deficient mice that have an autoimmune inflammatory disorder, suggesting that fibrotic lesions in those mice are a response to inflammation and not dependent upon the presence of TGF-β1. Recently, Nakajima and group (60) generated transgenic mice with elevated levels of activated TGF-β1 in the heart. This group observed overt fibrosis only in the atria and an inhibition of ventricular fibroblast DNA synthesis, suggesting that TGF-β1 activity is insufficient to promote ventricular fibrosis (60).

The recapitulation of fetal isoforms of cardiac genes (i.e., *β-Mhc*, *α-actins*) has historically been used as an indicator of cardiac hypertrophy (61–64). In fact, growth factors, including TGF-β1, have been

implicated in regulating the expression of fetal cardiac genes as seen with pressure overload hypertrophy (25, 65–67). However, there is a small but growing body of evidence that cardiac hypertrophy can be dissociated from the re-expression of embryonic isoforms of myofibrillar protein genes (26, 54, 68–72). Previously, we clearly demonstrated using FGF-2–deficient mice that the degree of hypertrophy did not influence the isoform switch of *Mhc* mRNA and protein since these mice had much less cardiac hypertrophy, yet the isoform switch from α- to β-MHC protein still occurred normally following pressure overload (26). In the present study, there was no isoform switch in MHC isoforms in saline- or subpressor Ang II–treated *Tgfb1*$^{+/+}$*Rag1*$^{-/-}$ and *Tgfb1*$^{-/-}$*Rag1*$^{-/-}$ mice, although *Tgfb1*$^{+/+}$*Rag1*$^{-/-}$ mice had a significant degree of cardiac hypertrophy (Figure 5). These data indicate that the MHC isoform switch occurs independently of the degree of hypertrophy, which is consistent with the notion that it is the burden of load that triggers the isoform switch (Figure 5). Others (69, 73) have also shown that the MHC isoform switch is dependent on pressure overload. Finally, using subpressor and pressor doses of Ang II, Susic and colleagues (69) demonstrated that an Ang II–induced increase in LV mass was not the result of pressure overload, whereas the isoform switch in LV *Mhc* mRNA was.

Anf expression levels were also determined in the present study and showed that Ang II–treated *Tgfb1*$^{+/+}$*Rag1*$^{-/-}$ mice, which were hypertrophic, had approximately a six-fold increase in cardiac *Anf* expression compared with saline-treated cohorts. However, a no-fold increase occurred in Ang II–treated *Tgfb1*$^{-/-}$*Rag1*$^{-/-}$ mice compared with their saline-treated cohorts. *Anf* expression has been shown to be elevated in forms of pathological cardiac hypertrophy, but not physiological hypertrophy (54, 55) and is used as a sensitive biomarker for the induction of the hypertrophic phenotype (see review, ref. 53).

In summary, our results demonstrate, we believe for the first time, an in vivo, functional role and direct effect of TGF-β1 in Ang II–induced cardiac hypertrophy. This effect is independent of an endogenously activated RAS or hemodynamic load. Surprisingly, the absence of TGF-β1 did not alter the level of fibrosis in this model. The α- to β-MHC isoform switch was dissociated from the hypertrophic growth of the heart, suggesting that mechanisms such as pressure overload, rather than cardiac hypertrophy, induce the re-expression of the fetal cardiac gene profile. Overall, our findings may provide a better understanding of the mechanism(s) of cardiac remodeling and new insight into the development of novel therapeutic strategies in cardiac hypertrophy.

Acknowledgments

This work was supported by grants from the NIH (HL-41496, HL-58511, HD-26470). The investigators acknowledge D. Puthoff for assistance with echocardiographic data; I.E. Ormsby for her excellent animal husbandry work; J.N. Lorenz for the use of blood pressure and flame photometry equipment; G.P. Boivin for pathological reports and for assistance with using the morphometric NIH imaging system; K. Hepner-Goss for assistance with using the fluorescence imaging system; Z. Spicer and D. Millhorn for expert scientific knowledge and technical assistance with the real-time PCR methodology, and R. Banks for critical review of the urinary aldosterone and Na^+ data and manuscript.

1. Massague, J. 1990. The transforming growth factor-beta family. *Annu. Rev. Cell Biol.* **6**:597–641.
2. Brand, T., and Schneider, M.D. 1995. The TGF beta superfamily in myocardium: ligands, receptors, transduction, and function. *J. Mol. Cell Cardiol.* **27**:5–18.
3. Kallapur, S., Ormsby, I., and Doetschman, T. 1999. Strain dependency of TGFbeta1 function during embryogenesis. *Mol. Reprod. Dev.* **52**:341–349.
4. Dickson, M.C., et al. 1995. Defective haematopoiesis and vasculogenesis in transforming growth factor-beta 1 knock out mice. *Development.* **121**:1845–1854.
5. Shull, M.M., et al. 1992. Targeted disruption of the mouse transforming growth factor-beta 1 gene results in multifocal inflammatory disease. *Nature.* **359**:693–699.
6. Kulkarni, A.B., et al. 1993. Transforming growth factor beta 1 null mutation in mice causes excessive inflammatory response and early death. *Proc. Natl. Acad. Sci. USA.* **90**:770–774.
7. Diebold, R.J., et al. 1995. Early-onset multifocal inflammation in the transforming growth factor beta 1-null mouse is lymphocyte mediated. *Proc. Natl. Acad. Sci. USA.* **92**:12215–12229.
8. D'Souza, R.N., and Litz, M. 1995. Analysis of tooth development in mice bearing a TGF-beta 1 null mutation. *Connect. Tissue Res.* **32**:41–46.
9. Glick, A.B., et al. 1996. Transforming growth factor beta 1 suppresses genomic instability independent of a G1 arrest, p53, and Rb. *Cancer Res.* **56**:3645–3650.
10. Hoying, J.B., et al. 1999. Transforming growth factor beta1 enhances platelet aggregation through a non-transcriptional effect on the fibrinogen receptor. *J. Biol. Chem.* **274**:31008–31013.
11. Tang, B., et al. 1998. Transforming growth factor-beta1 is a new form of tumor suppressor with true haploid insufficiency. *Nat. Med.* **4**:802–807.
12. Glick, A.B., et al. 1994. Targeted deletion of the TGF-beta 1 gene causes rapid progression to squamous cell carcinoma. *Genes Dev.* **8**:2429–2440.
13. Engle, S.J., et al. 1999. Transforming growth factor beta1 suppresses nonmetastatic colon cancer at an early stage of tumorigenesis. *Cancer Res.* **59**:3379–3386.
14. Thompson, N.L., et al. 1988. Transforming growth factor beta-1 in acute myocardial infarction in rats. *Growth Factors.* **1**:91–99.
15. Eghbali, M. 1989. Cellular origin and distribution of transforming growth factor-beta in the normal rat myocardium. *Cell Tissue Res.* **256**:553–558.
16. Takahashi, N., et al. 1994. Hypertrophic stimuli induce transforming growth factor-beta 1 expression in rat ventricular myocytes. *J. Clin. Invest.* **94**:1470–1476.
17. Li, R.K., et al. 1997. Overexpression of transforming growth factor-beta1 and insulin-like growth factor-I in patients with idiopathic hypertrophic cardiomyopathy. *Circulation.* **96**:874–881.
18. Li, G., et al. 1998. Elevated insulin-like growth factor-I and transforming growth factor- beta 1 and their receptors in patients with idiopathic hypertrophic obstructive cardiomyopathy. A possible mechanism. *Circulation.* **98**(Suppl. 19):II144–II149.
19. Millan, F.A., Denhez, F., Kondaiah, P., and Akhurst, R.J. 1991. Embryonic gene expression patterns of TGF beta 1, beta 2 and beta 3 suggest different developmental functions in vivo. *Development.* **111**:131–143.
20. Pelton, R.W., Saxena, B., Jones, M., Moses, H.L., and Gold, L.I. 1991. Immunohistochemical localization of TGF beta 1, TGF beta 2, and TGF beta 3 in the mouse embryo: expression patterns suggest multiple roles during embryonic development. *J. Cell Biol.* **115**:1091–1105.
21. MacLellan, W.R., Brand, T., and Schneider, M.D. 1993. Transforming growth factor-beta in cardiac ontogeny and adaptation. *Circ. Res.* **73**:783–791.
22. Eghbali, M., Tomek, R., Sukhatme, V.P., Woods, C., and Bhambi, B. 1991. Differential effects of transforming growth factor-beta 1 and phorbol myristate acetate on cardiac fibroblasts. Regulation of fibrillar collagen mRNAs and expression of early transcription factors. *Circ. Res.* **69**:483–490.
23. Villarreal, F.J., and Dillmann, W.H. 1992. Cardiac hypertrophy-induced changes in mRNA levels for TGF-beta 1, fibronectin, and collagen. *Am. J. Physiol.* **262**:H1861–H1866.
24. Kupfahl, C., et al. 2000. Angiotensin II directly increases transforming growth factor beta1 and osteopontin and indirectly affects collagen mRNA expression in the human heart. *Cardiovasc. Res.* **46**:463–475.

25. Parker, T.G., Packer, S.E., and Schneider, M.D. 1990. Peptide growth factors can provoke "fetal" contractile protein gene expression in rat cardiac myocytes. *J. Clin. Invest.* **85**:507–514.
26. Schultz, J.E., et al. 1999. Fibroblast growth factor-2 mediates pressure-induced hypertrophic response. *J. Clin. Invest.* **104**:709–719.
27. Tiret, L., et al. 2000. Lack of association between polymorphisms of eight candidate genes and idiopathic dilated cardiomyopathy: the CARDIGENE study. *J. Am. Coll. Cardiol.* **35**:29–35.
28. Patel, R., et al. 2000. Variants of trophic factors and expression of cardiac hypertrophy in patients with hypertrophic cardiomyopathy. *J. Mol. Cell. Cardiol.* **32**:2369–2377.
29. Gray, M.O., Long, C.S., Kalinyak, J.E., Li, H.T., and Karliner, J.S. 1998. Angiotensin II stimulates cardiac myocyte hypertrophy via paracrine release of TGF-beta 1 and endothelin-1 from fibroblasts. *Cardiovasc. Res.* **40**:352–363.
30. Lee, A.A., Dillmann, W.H., McCulloch, A.D., and Villarreal, F.J. 1995. Angiotensin II stimulates the autocrine production of transforming growth factor-beta 1 in adult rat cardiac fibroblasts. *J. Mol. Cell Cardiol.* **27**:2347–2357.
31. Sadoshima, J., and Izumo, S. 1993. Molecular characterization of angiotensin II-induced hypertrophy of cardiac myocytes and hyperplasia of cardiac fibroblasts. Critical role of the AT1 receptor subtype. *Circ. Res.* **73**:413–423.
32. Everett, A.D., Tufro-McReddie, A., Fisher, A., and Gomez, R.A. 1994. Angiotensin receptor regulates cardiac hypertrophy and transforming growth factor-beta 1 expression. *Hypertension*. **23**:587–592.
33. Ichihara, S., et al. 2001. Angiotensin II type 2 receptor is essential for left ventricular hypertrophy and cardiac fibrosis in chronic angiotensin II-induced hypertension. *Circulation*. **104**:346–351.
34. Schatz, D.G., Oettinger, M.A., and Baltimore, D. 1989. The V(D)J recombination activating gene, RAG-1. *Cell*. **59**:1035–1048.
35. Harada, K., et al. 1998. Pressure overload induces cardiac hypertrophy in angiotensin II type 1A receptor knockout mice. *Circulation*. **97**:1952–1959.
36. Williams, R.V., et al. 1998. End-systolic stress-velocity and pressure-dimension relationships by transthoracic echocardiography in mice. *Am. J. Physiol.* **274**:H1828–H1835.
37. Sahn, D.J., DeMaria, A., Kisslo, J., and Weyman, A. 1978. Recommendations regarding quantitation in M-mode echocardiography: results of a survey of echocardiographic measurements. *Circulation*. **58**:1072–1083.
38. Thoss, K., and Roth, J. 1977. The use of fluorescein isothiocyanate labeled lectins for immuno-histological demonstration of saccharides. III. Studies by use of *Ricinus communis* lectin and wheat germ agglutinin. *Exp. Pathol. (Jena)*. **14**:215–219.
39. D'Angelo, D.D., et al. 1997. Transgenic Galphaq overexpression induces cardiac contractile failure in mice. *Proc. Natl. Acad. Sci. USA*. **94**:8121–8126.
40. Seta, K.A., Kim, R., Kim, H.W., Millhorn, D.E., and Beitner-Johnson, D. 2001. Hypoxia-induced regulation of MAPK phosphatase-1 as identified by subtractive suppression hybridization and cDNA microarray analysis. *J. Biol. Chem.* **276**:44405–44412.
41. Reiser, P.J., and Kline, W.O. 1998. Electrophoretic separation and quantitation of cardiac myosin heavy chain isoforms in eight mammalian species. *Am. J. Physiol.* **274**:H1048–H1053.
42. Rogers, W.J., et al. 1975. Comparison of indices of muscle and pump performance in patients with coronary artery disease. *Cathet. Cardiovasc. Diagn.* **1**:17–34.
43. Osher, J., et al. 1976. Methylprednisolone treatment in acute myocardial infarction. Effect on regional and global myocardial function. *Am. J. Cardiol.* **37**:564–571.
44. Wood, M.A., Ellenbogen, K.A., Kapadia, K., Lu, B., and Valenta, H. 1990. Comparison of right ventricular impedance, pulse pressure and maximal dP/dt for determination of hemodynamic stability of ventricular arrhythmias associated with coronary artery disease. *Am. J. Cardiol.* **66**:575–582.
45. Bolognesi, R., et al. 2001. Detection of early abnormalities of left ventricular function by hemodynamic, echo-tissue Doppler imaging, and mitral Doppler flow techniques in patients with coronary artery disease and normal ejection fraction. *J. Am. Soc. Echocardiogr.* **14**:764–772.
46. Boivin, G.P., et al. 1995. Onset and progression of pathological lesions in transforming growth factor-beta 1-deficient mice. *Am. J. Pathol.* **146**:276–288.
47. Kulkarni, A.B., et al. 1995. Transforming growth factor-beta 1 null mice. An animal model for inflammatory disorders. *Am. J. Pathol.* **146**:264–275.
48. Brody, M.J. 1981. New developments in our knowledge of blood pressure regulation. *Fed. Proc.* **40**:2257–2261.
49. Reid, I.A. 1984. Actions of angiotensin II on the brain: mechanisms and physiologic role. *Am. J. Physiol.* **246**:F533–F543.
50. Yang, G., Wan, Y., and Zhu, Y. 1996. Angiotensin II—an important stress hormone. *Biol. Signals.* **5**:1–8.
51. Chan, J.C. 1979. Control of aldosterone secretion. *Nephron*. **23**:79–83.
52. Garty, H. 2000. Regulation of the epithelial Na+ channel by aldosterone: open questions and emerging answers. *Kidney Int.* **57**:1270–1276.
53. Silberbach, M., and Roberts, C.T., Jr. 2001. Natriuretic peptide signalling: molecular and cellular pathways to growth regulation. *Cell Signal.* **13**:221–231.
54. Buttrick, P.M., Kaplan, M., Leinwand, L.A., and Scheuer, J. 1994. Alterations in gene expression in the rat heart after chronic pathological and physiological loads. *J. Mol. Cell Cardiol.* **26**:61–67.
55. Calderone, A., Murphy, R.J., Lavoie, J., Colombo, F., and Beliveau, L. 2001. TGF-beta(1) and prepro-ANP mRNAs are differentially regulated in exercise-induced cardiac hypertrophy. *J. Appl. Physiol.* **91**:771–776.
56. Ruwhof, C., van Wamel, A.E., Egas, J.M., and van der Laarse, A. 2000. Cyclic stretch induces the release of growth promoting factors from cultured neonatal cardiomyocytes and cardiac fibroblasts. *Mol. Cell Biochem.* **208**:89–98.
57. Kim, N.N., Villarreal, F.J., Printz, M.P., Lee, A.A., and Dillmann, W.H. 1995. Trophic effects of angiotensin II on neonatal rat cardiac myocytes are mediated by cardiac fibroblasts. *Am. J. Physiol.* **269**:E426–E437.
58. Knowles, J.W., et al. 2001. Pressure-independent enhancement of cardiac hypertrophy in natriuretic peptide receptor A-deficient mice. *J. Clin. Invest.* **107**:975–984.
59. Omura, T., Kim, S., Takeuchi, K., Iwao, H., and Takeda, T. 1994. Transforming growth factor beta 1 and extracellular matrix gene expression in isoprenaline induced cardiac hypertrophy: effects of inhibition of the renin-angiotensin system. *Cardiovasc. Res.* **28**:1835–1842.
60. Nakajima, H., et al. 2000. Atrial but not ventricular fibrosis in mice expressing a mutant transforming growth factor-beta(1) transgene in the heart. *Circ. Res.* **86**:571–579.
61. Lompre, A.M., et al. 1979. Myosin isoenzyme redistribution in chronic heart overload. *Nature*. **282**:105–107.
62. Mercadier, J.J., et al. 1981. Myosin isoenzyme changes in several models of rat cardiac hypertrophy. *Circ. Res.* **49**:525–532.
63. Tsuchimochi, H., et al. 1984. Isozymic changes in myosin of human atrial myocardium induced by overload. Immunohistochemical study using monoclonal antibodies. *J. Clin. Invest.* **74**:662–665.
64. Lompre, A.M., Mercadier, J.J., and Schwartz, K. 1991. Changes in gene expression during cardiac growth. *Int. Rev. Cytol.* **124**:137–186.
65. Schneider, M.D., and Parker, T.G. 1990. Cardiac myocytes as targets for the action of peptide growth factors. *Circulation*. **81**:1443–1456.
66. Parker, T.G., and Schneider, M.D. 1991. Growth factors, proto-oncogenes, and plasticity of the cardiac phenotype. *Annu. Rev. Physiol.* **53**:179–200.
67. Parker, T.G., Chow, K.L., Schwartz, R.J., and Schneider, M.D. 1991. TGF-beta 1 and fibroblast growth factors selectively up-regulate tissue-specific fetal genes in cardiac muscle cells. *Ciba Found. Symp.* **157**:152–160.
68. Mercadier, J.J., et al. 1983. Myosin isoenzymes in normal and hypertrophied human ventricular myocardium. *Circ. Res.* **53**:52–62.
69. Susic, D., Nunez, E., Frohlich, E.D., and Prakash, O. 1996. Angiotensin II increases left ventricular mass without affecting myosin isoform mRNAs. *Hypertension*. **28**:265–268.
70. Bauer, E.P., Kuki, S., Zimmermann, R., and Schaper, W. 1998. Upregulated and downregulated transcription of myocardial genes after pulmonary artery banding in pigs. *Ann. Thorac. Surg.* **66**:527–531.
71. Vikstrom, K.L., Bohlmeyer, T., Factor, S.M., and Leinwand, L.A. 1998. Hypertrophy, pathology, and molecular markers of cardiac pathogenesis. *Circ. Res.* **82**:773–778.
72. Sadoshima, J., and Izumo, S. 1995. Rapamycin selectively inhibits angiotensin II-induced increase in protein synthesis in cardiac myocytes in vitro. Potential role of 70-kD S6 kinase in angiotensin II-induced cardiac hypertrophy. *Circ. Res.* **77**:1040–1052.
73. Izumo, S., et al. 1987. Myosin heavy chain messenger RNA and protein isoform transitions during cardiac hypertrophy. Interaction between hemodynamic and thyroid hormone-induced signals. *J. Clin. Invest.* **79**:970–977.